Comparing different rock mass classifications using field and point cloud data on a rock cut

Dragana Slavković
Institute of Transportation CIP, Belgrade, Serbia

Aljoša Mitić
Central road laboratory CPL, Novi Sad, Serbia

Miloš Marjanović
University of Belgrade, Faculty of Mining and Geology, Belgrade, Serbia

ABSTRACT: Classifying rock masses implies a systematic quantification of various field data, lately including point clouds acquired using LiDAR or photogrammetric techniques. They have been proven useful for extraction of additional information and more confident rock mass classification in inaccessible parts of the slope. In this work, a rock cut along the railway Knjaževac – Zaječar in Serbia was analyzed using conventional field mapping and data extracted from point clouds. Basic RMR, SMR and Q-slope classifications were used for rock mass characterization. Extraction from the point cloud was applied beyond the accessibility line (>2 m), and included determination of *RQD*, joint spacing and orientation. The rock mass is split into three zones, wherein RMR score equaled 64, 57, and 56 for Zone 1, 2 and 3, respectively, whereas SMR score equaled 49, 42, and 41, respectively. A better distinction between the zones was achieved using Q-slope score, totaling 1.75, 0.66 and 0.31, respectively.

Keywords: Rock Mass Classifications, RMR, SMR, Q-slope, LiDAR.

1 INTRODUCTION

Rock mass classification systems were designed to act as an engineering design aid, commonly resulting in a single numerical value, interval, or category that well describes subject rock material. It is no alternative to field observations, analytical considerations, measurements, and engineering judgment, but rather their extension (Hoek & Bray, 1981). To choose among different systems is not as straightforward as it seems. It is recommendable to use the basic Rock Mass Rating (RMR), in parallel with at least one additional system. In this work RMR, together with Slope Mass Rating (SMR) and Q-slope classification system were used and cross-compared. To this end Light Detection and Ranging (LiDAR) based point cloud was used to provide better support while scoring standard rock mass parameters. The way of quantifying and adopting the value of certain rock mass parameters, as well as the overall rating of the rock mass classification, largely depends on the experience of the interpreter. Therefore, combining several methodological approaches during quality assessment of the rock mass and its stability is desirable, especially if, as in this case, the additional methodological approach is based on 3D data.

2 ROCK MASS CLASSIFICATION RETROSPECTIVE

One of the foremost and the most widespread, used in all kinds of applications, starting from tunneling to slopes and cuts, is the RMR classification system, which has endured several upgrades since the original version. The latest version (Bieniawski, 1989) was used as a base in this work during site investigations. Since it is one of the best-known systems it is not going to be described hereinafter, but a brief overview of other systems used will follow.

Another classical lump-rating classification system specialized for rock slopes is the SMR (Romana, 1985), which is derived from the RMR system by appending adjustment parameters for discontinuity orientations in relation to the slope attitude, as well as the effect of the excavation method, as expressed in the following equation:

$$SMR = RMR_{\mathrm{b}} + (F_1 \cdot F_2 \cdot F_3) + F_4 \tag{1}$$

wherein, RMR_b is the RMR value determined from the RMR version from 1989 without considering the impact of discontinuity orientation; F_1 is an adjustment factor, which depends on the parallelism between the joint (planar failure) or joint intersection (wedge failure) strike (α_j) on one side and the slope face strike (α_s) on the other; F_2 refers to joint dip angle or the according intersection line (β_j); F_3 reflects the effect of the angle between the slope face dip (β_s) and the joint dip or the according intersection line plunge (β_j); F_4 is an adjustment factor that depends on the excavation method.

Q-slope is another classification system applied in this work, and it represents an empirical rock slope engineering method for assessing the stability of excavated rock slopes in the field (Bar & Barton, 2017). It is practically impossible to assess the stability of rock slope cuttings in real time, using analytical approaches such as kinematics, limit equilibrium, or FEM/DEM modeling. However, this classification system can be very useful because it allows a quick assessment of the unsupported slopes stability depending on their slope angle. The numerical value of the Q index varies on a logarithmic scale from 0.001 to a maximum of 100 as defined by:

$$Q_{slope} = \frac{RQD}{J_n} \cdot \left(\frac{J_r}{J_a}\right)_0 \cdot \frac{J_{wice}}{SRF_{slope}} \tag{2}$$

wherein, RQD is the rock quality designator, J_n is the joint sets number, J_r is the joint roughness number, J_a is the joint alteration number, J_{wice} is an environmental and geological condition number, SRF_{slope} represent three strength reduction factors a, b and c ($SRFa$ is the physical condition number, b is the stress and strength number, and c is the major discontinuity number) and O-factor is the orientation factor for the ratio J_r/J_a.

The first quotient (RQD/J_n) representing the structure of the rock mass, is a crude measure of the block or particle size. The second quotient (J_r/J_a) represents the roughness and frictional characteristics of the joint walls or filling materials. The third quotient (J_{wice}/SRF_{slope}) represents the external factors and stress affecting the rock mass. The discontinuity orientation factor (O-factor) provides orientation adjustments for discontinuities in rock slopes. The strength reduction factor SRF_{slope} is obtained by using the most adverse i.e., maximum of the $SRFa$, $SRFb$, and $SRFc$.

3 POINT CLOUD APPLICATION IN ROCKSLOPE ENGINEERING

In addition to the conventional procedure of collecting discontinuity data in the field, the LiDAR technique is lately becoming increasingly popular. The basic laser scanning output is a point cloud, a discrete 3D model of terrain surface represented by points defined by three relative or referenced coordinates.

Some rock mass characterization and analyses can be performed directly on a point cloud (or a sequence of point clouds): discontinuity tracing, rock mass and discontinuity characterization (number of sets, orientation of daylight planes, joint spacing, block size and shape, joint persistence), rock slope monitoring, 3D rockfall simulation (back-analysis), rockfall hazard (prediction of future events and their magnitudes). If the point cloud is recorded with a high resolution, then roughness,

water condition and aperture can also be defined. Parameters that are very difficult or impossible to define through a point cloud are rock type and state of weathering, as well as field/lab test properties (Marjanović et al, 2022). Kinematic analysis can also be routinely performed assuming that the slope accurately fits the point cloud and that the essential discontinuity systems are visible on the slope face (Jaboyedoff et al., 2007). Pre-failure deformations that can predict which parts of the slope are most vulnerable are also in experimental practice (Marjanović et al, 2021).

4 CASE STUDY – RAILWAY CUT KNJAŽEVAC-ZAJEČAR

Local instabilities that can threat railway traffic are reported on the railway Crveni krst – Prahovo Pristanište (in vicinity of the town of Knjaževac in eastern Serbia), along chainage km 59+185 to km 59+220 where a 10 m high rock cut aligns to the railway for about 40 m in length. The first incident was witnessed in 1988, and since no remedial measures were undertaken, the process intensified onward. The Institute of Transportation "CIP" from Belgrade performed field mapping and 3D terrestrial laser scanning of the rock slope in 2017, while the site was revisited for additional logging and scanning in May 2022.

The wider area around the site is composed of several distinctive units. The Lower Cretaceous unit ($K_1^{3,4}$) is separated into two facies with pure carbonates (shallow-water) or marly-siltstone sediments (deep-water). Both facies are mostly layered, banked or massive. They are made of massive limestone, thin-layered to plate-like limestone slightly marly-sandy, marly-sandy to lumpy limestones, and clayey limestones alternating in irregular succession. These limestone facies drastically differ in strength within the railway rock cut. They are divided by joint sets influenced by external forces (frost, physical-chemical weathering, plants growth, etc.). The influence of water on the cut is reflected in dissolution of carbonates, washing-out of clay particles and the frost-dynamic effect. The softest clayey limestones are almost completely disintegrated near the surface, while the hardest parts comprise of pure carbonate limestone blocks. Karstification is not clearly expressed.

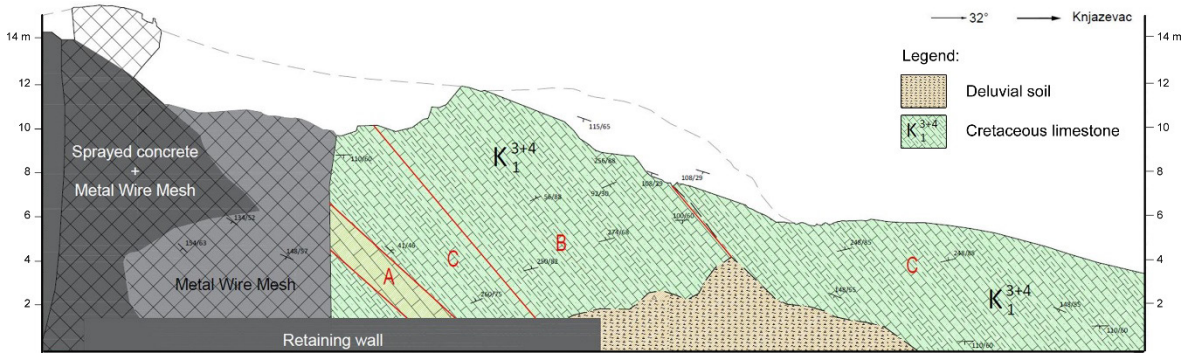

Figure 1. Engineering geological section with separated geotechnical zones A, B & C.

Engineering geological mapping (Fig. 1) of the rock cut face was carried out along 35 m (at chainage from km 59+185 to km 59+220), using the classic procedure, in places that are accessible, up to about 2 m in height, at the lower parts of the cut and above newly installed retaining wall. It included determination of slope angle, number of discontinuity sets, measurement of their orientations, joint spacing, persistence, roughness, joint wall strength and aperture, observation of physical and chemical changes on the slope and possible presence of joint filling. The condition of the slope face and the observation of potential zones of instability was determined by a visual inspection of the slope and based on earlier mapping, while the mapping was completed by dividing the slope into three geotechnical zones: A, B and C. Zone A represents a geotechnical class with the best mechanical properties, while Zone C is with the weakest.

Terrestrial scanning was carried out using LiDAR technology, using both Leica ScanStation P20 professional scanner in 2017, as well as an iPadMaxPro device in 2020. The scanning with the professional scanner was carried out along a wider section, wherein the subject 35 m cut is just a segment. The rescanning with the tablet device was targeted at specific details, i.e., critical portions

of the subject rock cut. The tablet-based scanning included 18 recordings, 9 of which were in low resolution and the other 9 were recorded in high resolution. Each of the recordings covers a maximum span of about 10 m in length and about 4 m in height. The resulting point clouds were used directly to measure RQD under desired scan lines, orientations of the inaccessible discontinuity faces, joint spacing and persistence. This data was appended to field logs to achieve higher certainty in the rock mass classification process (Fig. 2).

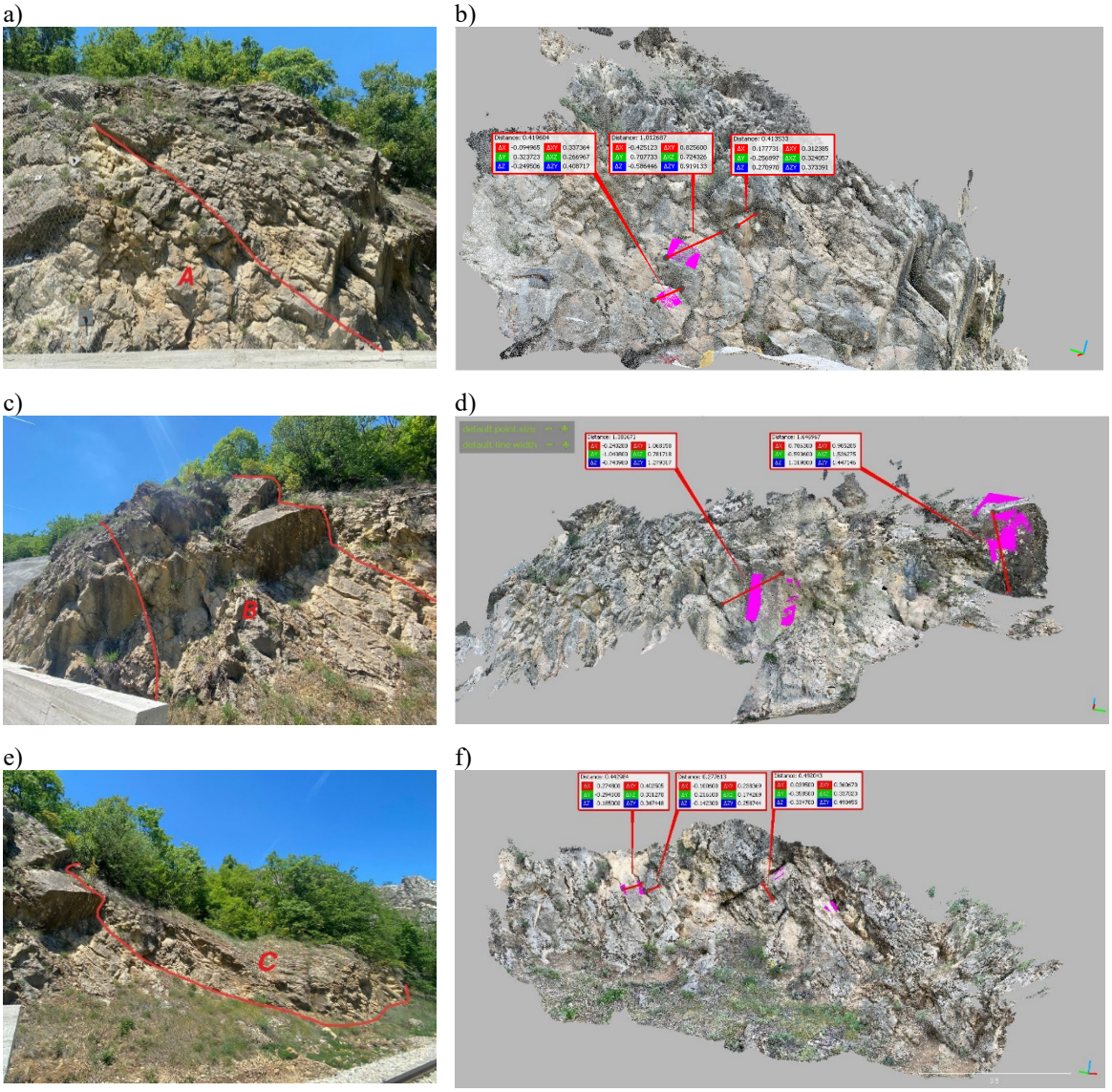

Figure 2. Geotechnical zones and their point cloud counterparts with examples of data extraction (spacing as red lines, orientation and persistence as purple polygons): a) Zone A in the field; b) Zone A on a point cloud; c) Zone B in the field; d) Zone B on a point cloud; e) Zone C in the field; f) Zone C on a point cloud.

5 RESULTS

The rock mass within designated zones was classified against all three proposed systems, basic RMR_{89}, SMR, and Q-slope. The summary of collected data from both field investigation and additional point cloud measurements is given in Table 1. Notably, the final scores are discernable but not drastically different as would be expected from the subject rock material, especially between Zone B and C. Clearly, the engineering judgement to separate the rock mass into designated zones would not find much justification under basic RMR_{89} system.

Table 1. Rock Mass Rating System without effect of discontinuity orientation (scores in parentheses).

Zone		A	B	C
UCS of intact rock*	[MPa]	~ 107 (8)	~ 75 (6)	~ 60 (5)
Drill Core Quality *RQD*	[%]	75 – 90 (17)	60 – 80 (14)	40 – 60 (10)
Spacing of discontinuities	[m]	0.25 – 0.75 (10)	0.30 – 0.75 (9)	0.10 – 5.00 (11)
Persistence	[m]	12.2 (1)	11.5 (1)	8.6 (2)
Separation	[mm]	2.2 (1)	6.2 (0)	4.3 (1)
Roughness	[-]	slightly (4)	slightly (4)	slightly (4)
Infilling	[-]	missing (6)	missing (6)	missing (6)
Weathering	[-]	moderately (4)	moderately (4)	moderately (4)
Groundwater	[-]	almost dry (13)	almost dry (13)	almost dry (13)
RMR_{89} = Σ without effect of discontinuity orientation		64	57	56

*Unconfined compressive strength obtained by PLT tests, using UCS=24xI_s.

Table 2. SMR classification system and following results (scores in parentheses).

Zone		A	B	C
RMR_b		(64)	(57)	(56)
Orientation α_j/α_s	[°]	208/32	210/32	210/32
$F_1 = (\alpha_j-\alpha_s-180°)$		(1)	(1)	(1)
Orientation β_j	[°]	45	55	65
$F_2 = \beta_j$		(1)	(1)	(1)
Orientation β_s	[°]	76	70	76
Toppling – type failure F				
$F_3 = (\beta_j + \beta_s)$		(-25)	(-25)	(-25)
F_4 *(Pre-splitting)*		(10)	(10)	(10)
Σ SMR		*Partially stable* 49	*Partially stable* 42	*Partially stable* 41

Table 3. Q-slope classification system and following results (scores in parentheses).

Zone	A	B	C
RQD [%]	75 – 90 (80)	60 – 80 (70)	40 – 60 (50)
J_n	*3 joint sets + random joints* (12)	*3 joint sets + random joints* (12)	*4 or more joint sets* (15)
J_r	*Rough or irregular, undulating walls of joints* (3)	*Rough or irregular, undulating walls of joints* (3)	*Rough or irregular, undulating walls of joints* (3)
J_a	*Unaltered joint walls, surface staining only* (1)	*Slightly altered joint walls. Non-softening mineral coatings* (2)	*Slightly altered joint walls. Non-softening mineral coatings* (2)
O - factor	*Very unfavorable orientation* (0.5)	*Very unfavorable orientation* (0.5)	*Very unfavorable orientation* (0.5)
J_{wice}	*Wet environment: Stable structure / competent rock* (0.7)	*Wet environment: Stable structure / incompetent rock* (0.6)	*Wet environment: Unstable structure / competent rock* (0.5)
SRF_{slope}	*Very unfavorable major discontinuity with little or no clay* (4)	*Very unfavorable major discontinuity with little or no clay* (4)	*Very unfavorable major discontinuity with little or no clay* (4)
Σ Q-slope	1.75	0.66	0.31

The SMR value was obtained by calculating the factors F_1, F_2, F_3 and F_4, and using the RMR_{89} value (rating without effect of discontinuity orientation), and the results are shown in Table 2. The discrepancy between the zones is even smaller than in the basic RMR_{89} case, as all spatial factors turn out to be the same, while such outcome was expected for the F4, since same blasting conditions apply to the entire cut. All three zones came out as Partially stable, Zone B and C marginally, but nevertheless within the same SMR class. Arguably, the engineering judgement would imply that Zone C is a significantly poorer rock mass, that needs to fall at least one class under Zones B and A.

Finally, the Q-slope results, which are presented in Table 3. suggest better distinction between the three Zones. Zone A, with the highest score of 1.75, implying that rock mass would be stable under very steep angles of up to ~70°. In Zone B, with score of 0.66, the stability limit falls to ~60°, and in Zone C to ~55°. Given that slope locally exceeds these angles the stability is obviously compromised which matches the engineering judgement during the mapping process, as well as reported cases during the years, and therefore, best fits the engineering criteria.

6 CONCLUSIONS

This case study demonstrates a good combination of conventional and LiDAR based data extraction on a rock cut face, wherein several parameters, such as RQD, joint orientation, spacing and persistence, were significantly improved and densified by using appropriate point clouds. This was especially important for the inaccessible part. Even tablet device was proved useful as it can reach twice to three-times as high above the accessibility limit (~2 m). This technology becomes abundantly available and economic, easily portable, and can find purpose in aiding the mapping process for moderately high slopes and cuts. On the other hand, professional scanners can reach even higher and allow data extraction from almost entire slope face in this particular example, but succumbs to the higher costs (instrument cost, operational expenses, etc.).

All three selected classification systems equally benefited from using data extracted from the according point clouds. Yet, these effects were visible only in the case of Q-slope, wherein the classification score fits the expert engineering judgement, which led to initial separation into A, B and C zones. It is important to mention that such a conclusion applies to the subject rock slope and does not necessarily entail general recommendation. It remains the safest to practice several classification systems in parallel and compare them mutually and with other engineering tools available.

REFERENCES

Bar, N., & Barton, N. (2017). The Q-slope method for rock slope engineering. Rock Mechanics and Rock Engineering, 50, 3307-3322.

Bieniawski, Z. T. (1989). Engineering rock mass classifications: a complete manual for engineers and geologists in mining, civil, and petroleum engineering. John Wiley & Sons.

Hoek, E., & Bray, J. D. (1981). Rock slope engineering. CRC press, London, UK. 358.

Jaboyedoff, M., Metzger, R., Oppikofer, T., Couture, R., Derron, M. H., Locat, J., & Turmel, D. (2007, May). New insight techniques to analyze rock-slope relief using DEM and 3Dimaging cloud points: COLTOP-3D software. In 1st Canada-US Rock Mechanics Symposium. OnePetro.

Marjanović, M., Abolmasov, B., Berisavljević, Z., Pejić, M., & Vranić, P. (2021, August). Pre-failure deformation monitoring as rockfall prediction tool. In IOP Conference Series: Earth and Environmental Science (Vol. 833, No. 1, p. 012197). IOP Publishing.

Marjanović, M., Abolmasov, B., Đurić, U., Krušić, J., & Bogdanović, S. (2022). Regional rockfall exposure assessment, experiences from Serbia. In Proceedings of the 5th Regional Symposium on Landslides in the Adriatic-Balkan Region (pp. 145-150). Faculty of Civil Engineering, University of Rijeka.

Romana, M. (1985, September). New adjustment ratings for application of Bieniawski classification to slopes. In Proceedings of the international symposium on role of rock mechanics, Zacatecas, Mexico (pp. 49-53).